Valence One-Electron and Shake-Up Ionization Bands of Carbon Clusters. III. The C_n (n = 5,7,9,11) Rings

M. S. Deleuze,* M. G. Giuffreda, and J.-P. François

Limburgs Universitair Centrum, Institute for Materials Science (IMO), Departement SBG, Universitaire Campus, B-3590 Diepenbeek, Belgium

Received: November 30, 2001

The *1h* (one-hole) and *2h-1p* (two-hole; one-particle) shake-up bands in the valence ionization spectrum of odd-membered carbon rings (C_5, C_7, C_9, C_{11}) are investigated by means of the third-order algebraic diagrammatic construction [ADC(3)] scheme for the one-particle Green's function. Despite a severe dispersion of the σ- and π- ionization intensity over intricately dense sets of satellites, the present study undoubtedly confirms that structural fingerprints in ionization spectra could be usefully exploited to discriminate the cyclic C_5, C_7, C_9, and C_{11} species from their linear counterparts in plasma conditions. Such spectra could also be used to indirectly trace very fine details of the molecular structure, such as bond length alternations, out-of-plane distortions, or the strength of cyclic strains. Both structurally and electronically, the cyclic isomers of the C_5 and C_9 clusters must be described as even-twisted cumulenic tori, whereas the C_7 and C_{11} cyclic species are simply planar polyynic rings. In comparison with their linear counterparts, all species display an intrinsically lower propensity to electronic excitations, marked by a rather significant increase of the fundamental HOMO−LUMO band gap. On the other hand, the lower symmetry of the cyclic clusters, C_5 and C_9 in particular, permits many more configuration interactions in the cation. The ultimate outcome of these two opposite factors is, overall, a severe enhancement of the shake-up fragmentation of ionization bands, compared with the linear isomers.

I. Introduction

Carbon clusters have aroused great interest since their mass spectrographical detection in 1943 by Mattauch, Ewald, Hahn, and Strassmann. An historical sketch and a review of the vast literature of carbon-cluster research is presented in refs 1 and 2. Studies of C_n species are of relevance in astrophysics and, closer to our terrestrial concerns, in the fields of combustion processes and material sciences. These compounds indeed abound in interstellar clouds, comet tails, carbon stars, or the atmosphere of red-giant stars,[3] as well as in hydrocarbon flames and soots.[4] They are also assumed to be key intermediates in the growth of thin but ultra-hard diamond and silicon-carbide films via chemical vapor deposition.[5,6] The interest in carbon clusters has been boosted since the 1980s by the serendipitous discovery and dramatic emergence in material sciences of new allotropic forms of carbon, such as fullerenes and carbon nanotubes,[7,8] the formation of which proceeds through a condensation of small carbon chains or rings.[9]

One notoriously difficult and controversial area of carbon cluster research is that of structural analysis. Owing to the large flexibility of carbon with regard to chemical bonding, pure carbon molecules show a great diversity of structures comprising chains, monocyclic, bicylic, and polycyclic rings, graphite sheets or bowls, closed spheroidal cages or fullerenes, extended nanotubes,[1,2] and finally fullerene oligomers or polymers.[10] Strong evidences for the existence of small cyclic isomers (i.e., with a size ranging from C_4 to C_{18}) have been given by ab initio calculations,[11−19] ion mobility studies using gas-phase ion chromatography,[20] as well as from Coulomb explosion experiments in combination with laser photodetachment.[21] Two recent studies of odd-membered C_{2n+1} ($n = 1-4$) chains[22] and even-membered C_{2n} ($n = 2-5$) rings[23] have recently evidenced that much information on the structure of neutral carbon clusters could be gained from the measurement and characterization of their ionization spectra. A detailed study of adiabatic ionization processes and their outcomes on carbon clusters with a size ranging from C_4 to C_{19} has also been presented.[24] In continuation of these studies, the aim of the present work is to provide further reliable simulations of the *vertical* ionization spectra of the odd-membered C_{2n+1} ($n = 2-5$) cyclic carbon clusters in their singlet closed-shell ground state. A detailed study of these spectra is by its own of fundamental interest, with regard to the impact of cyclic molecular connectivities on the electronic structure.[25] More practically, the ionization spectra computed for such species could be usefully exploited at a later stage to experimentally follow the transition from the linear to the cyclic carbon clusters, which in terms of energy differences undubitously occurs from C_{10}.[11,14,15,19] However, the energy difference at the CCSD(T)/cc-pVDZ level between the cyclic and linear species drops[19c] with increasing cluster size from 56 kcal mol^{-1} for C_5, to 13 and 8 kcal mol^{-1} only for C_7 and C_9, respectively. For C_{11}, the ring structure has been prediced to be the most stable one by 29 kcal mol^{-1}.[19c] Most often, the production of carbon clusters implies considerable heating, and entropic effects can favor the cyclic species before C_{10}.[1,2]

Owing to their low energy band gap and their strongly correlated character, detailed calculations of the valence ionization spectra of carbon clusters are particularly challenging. To accurately describe one-electron binding energies and properly account for the secondary (satellite) structures, one must resort to theoretical methods which deal both with the effects of

* To whom correspondence should be addressed. E-mail: deleuze@luc.ac.be.

10.1021/jp014260u CCC: $22.00
Published on Web 05/18/2002

electron relaxation and correlation, as well as with multiconfiguration interactions in the final state. In the case of carbon clusters, the latter are strong enough to yield a severe breakdown of the orbital picture of ionization,[26] which leads to a dispersion of a major part of the ionization intensity over dense sets of low-intensity satellite (or, equivalently, shake-up) lines spreading down to outer-valence energies.[22,23] A widely available approach such as the Outer-Valence Green's Function method for the calculation of one-electron vertical ionization energies[27−29] can thus only be applied with great care, since it may perform very poorly when nearby shake-up lines are present, and we aim at a consistent and complete description of such lines too.

One of the most convenient tools for investigating valence one-electron and shake-up ionization bands is provided by the so-called[28,30−32] third-order Algebraic Diagrammatic Construction scheme [ADC(3)] of the one-particle Green's Function [1p-GF][33,34] (or, equivalently, one-electron propagator[35,36]). Briefly, in such a scheme, a secular matrix is cast over a set of primary (1p, 1h) and excited (shake-on, 2p-1h, or shake-up, 2h-1p) anion and cation states derived from the neutral molecular ground state. Diagonalization of the ADC(3) matrix enables a consistent description of these states through third- and first-order in electron correlation, respectively. Clearly, because of their low symmetry (C_2, C_{2v}), severe computational difficulties can be anticipated with applications of this scheme to the cyclic isomers of C_5, C_7, C_9, and C_{11}. These difficulties are well-known and arise from the size of the matrices to be diagonalized and from the large number of ionic states to be identified in order to secure a reliable assignment of shake-up bands. Indeed, regardless of the molecular symmetry point group, the number of shake-up states per occupied orbital in chains or rings $(-A-)_n$ of increasing size[22,23,37−43] grows proportionally to n^2, whereas their intensities scale on average like n^{-2}.[40,41] Further redistribution of ionization intensity in dense and complex shake-up sets occurs upon symmetry lowering.[38] Therefore, despite the advances seen over the last five years, an exhaustive study at the ADC(3) level of the ionization spectrum of a compound like C_9 still clearly amounts to a "*tour de force*", when considering its very limited (C_2) symmetry.

Besides the ADC(3) computations, for comparison purposes and in order to bracket errors due to the limitations of the basis sets used, and since the ionization spectra of the C_{2n+1} (n = 5) cyclic carbon clusters have never been investigated, we also undertake large basis set OVGF computations of the outermost one-electron ionization states of these species.

II. Methodological Details

The geometries of the cyclic C_5, C_7, C_9, and C_{11} clusters have been optimized[19] using Density Functional Theory (DFT)[44] together with the Becke's three-parameter Lee−Yang−Parr (B3LYP)[45] hybrid functional. The DFT(B3LYP) computations have been carried out in conjunction with Dunning's correlation consistent polarized valence double-ζ (cc-pVDZ) basis set.[46] As pointed out in previous studies,[19,24,47] the B3LYP/cc-pVDZ approach provides structural (as well as vibrational) results of quality comparable to those obtained at the CCSD(T)/cc-pVDZ level of theory, a benchmark level in quantum chemistry. The investigated structures are sketched in Figure 1.

Whenever possible, OVGF calculations of one-electron binding energies were carried out from the computed B3LYP/cc-pVDZ geometries using the GAUSSIAN98 package[48] with four basis sets, namely correlation-consistent polarized valence basis sets of double (cc-pVDZ), triple (cc-pVTZ) and quadruple (cc-pVQZ) ζ quality,[46] as well as with the augmented cc-pVDZ basis set.[49] The basis set dependence of the computed ADC(3) one-electron and shake-up ionization bands of carbon clusters has also been previously assessed by comparison with the results of 1p-GF/ADC(3)/cc-pVDZ and 1p-GF/ADC(3)/aug-cc-pVDZ calculations on the C_3 chain[22] and C_4 ring.[23] Improving the cc-pVDZ basis set by inclusion of diffuse functions was found to lead to a redistribution of intensities among shake-up lines, but merely without any significant alterations of the shape and location of bands, up to binding energies of 30 eV.

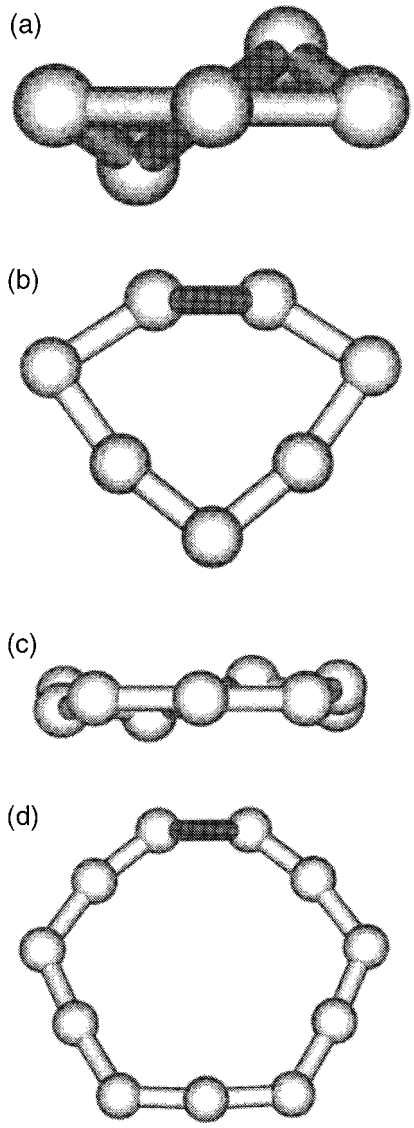

Figure 1. Molecular structures of the (a) C_5 (C_2), (b) C_7 (C_{2v}), (c) C_9 (C_2), and (d) C_{11} (C_{2v}) clusters (B3LYP/cc-pVDZ results).

For the sake of consistency with our previous investigations[22,23] on the linear C_{2n+1} (n = 1−4) and the cyclic C_{2n} (n = 2−5) species, the 1p-GF/ADC(3) calculations presented in this work are performed using Dunning's valence correlation-consistent polarized double zeta basis set (cc-pVDZ). The Hartree−Fock (HF) entries required for the 1p-GF/ADC(3) computations[50] have been obtained from SCF calculations carried out using the GAMESS−US series of programs.[51] The requested convergences on each element of the HF density matrix and the integral cutoff were fixed to 10^{-5} and 10^{-9} hartree, respectively. For the ADC(3) computations on C_5 and C_7, all ionization lines with a pole strength larger than 0.005 have been extracted through a block-Davidson diagonalization of the 1p-GF/ADC(3) secular matrix. For practical reasons, this

TABLE 1: Total RHF/cc-pVDZ Energies [E(RHF), in a.u.], Orbital Energies ϵ (in eV) and the Fundamental (HOMO−LUMO) Band Gap [ΔE_g (in eV)] of the Cyclic and Linear C_{2n+1} Clusters ($n = 1-4$)

	cyclic						linear					
		HOMO		LUMO				HOMO		LUMO		
species	E(RHF)	orbital	ϵ	orbital	ϵ	ΔE_g	E(RHF)	orbital	ϵ	orbital	ϵ	ΔE_g
C_5	−188.912607	7b	−11.006	9a	−0.335	10.672	−189.030966	$1\pi_g$	−10.947	$2\pi_u$	−1.295	9.652
C_7	−264.656705	$11a_1$	−9.512	$3b_1$	+0.280	9.802	−264.695601	$2\pi_u$	−9.980	$2\pi_g$	−1.844	8.136
C_9	−340.341661	13b	−9.066	15a	−0.845	8.221	−340.360956	$2\pi_g$	−9.342	$3\pi_u$	−2.208	7.134
C_{11}	−416.063520	$13b_2$	−8.263	$3a_2$	−0.825	7.438	−416.024941	$3\pi_u$	−8.886	$3\pi_g$	−2.470	6.416

threshold had to be increased to 0.02 in the case of C_9 and C_{11}. The spatial symmetry has been exploited to the extent of the molecular Abelian (C_2 or C_{2v}) point group.

The simulated spectra presented in the sequel are constructed from a convolution of the 1p-GF/ADC(3) ionization lines, using as spread function a linear combination of one Lorentzian and one Gaussian curve of equal weight and width (fwhm = 1.1 eV). The intensities are scaled according to the spectroscopic pole strengths. Despite the neglect of photoionization cross sections, this procedure provides very consistent insights into ultra-violet photoionization spectra of large and low band-gap compounds (see e.g., ref 43).

The interested reader is referred further to ref 22 and references therein, for a complete diagrammatic overview of the ADC(3) scheme and for detailed discussions of practical and essential aspects (*systematic compactness*, *size-consistency*, *size-intensivity*, *charge-consistency*,...) of this method with regard to applications on systems of increasing size.

III. Results and Discussion

A. Structural and Topological Considerations. Unlike their even-membered cyclic counterparts, for which the Hückel rules of (double) aromaticity and anti-aromaticity provides a simple qualitative explanation of the cumulenic and polyynic nature of the C_{2n+2} and C_{2n} species, respectively, odd-membered cyclic carbon clusters have rather peculiar structural properties. Cyclic compounds such as C_5 and C_9 exhibit very little bond length alternations, and as such can be regarded as cumulenic,[24] but at the same time exhibit (Figure 1) striking deviations from planarity.[19] On the other hand, the cyclic isomers of C_7 and C_{11} are planar[19] but polyynic[24] rings, characterized by rather pronounced bond length alternations and a completely different behavior upon adiabatic ionization.[24] Because electronic properties in general, and ionization energies in particular, are strongly sensitive to details of the molecular structure, a preliminary topological analysis of molecular orbitals is required before embarking on a quantitative investigation of ionization spectra. Basic characteristics such as the RHF total energy or orbital energies of the C_{2n+1} ($n = 2-5$) chains and rings are correspondingly listed in Table 1. If relative stabilities were to be inferred from this Table, it should be reminded that energy differences between carbon clusters are extremely sensitive to electron correlation (see e.g., refs 12, 13, 18, 19).

Considering that outermost orbitals have very generally a dominating impact on the total electron density and chemical bond orders, as well as on chemical reactivity, we reproduce in Figure 2 the highest occupied molecular orbitals (HOMO) of the odd-membered carbon chains and of their cyclic counterparts, in order to understand in detail the structural variations that occur upon ring closure, as well as their intricate interplay with electronic properties. The linear forms of odd-membered carbon clusters in their singlet ground state are cumulenic chains (see ref 24 and references therein), and as such possess as highest occupied level a doubly degenerate and perfectly

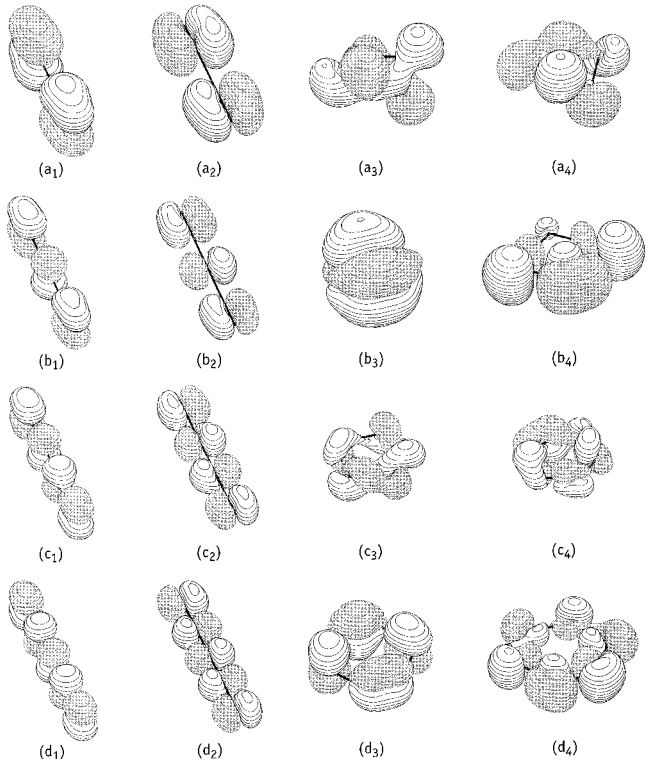

Figure 2. (a_1-d_1, a_2-d_2) Highest Occupied Molecular Orbitals (HOMO) of C_{2n+1} carbon chains versus the (a_3-d_3) HOMO-1 and (a_4-d_4) HOMO orbitals of the C_{2n+1} rings. (a): C_5 [a_1:$1\pi_g$, a_2:$1\pi_g$, a_3:8a, a_4:7b]; (b): C_7 [b_1:$2\pi_u$, b_2:$2\pi_u$, b_3:$2b_1$, b_4:$11a_1$]; (c): C_9 [c_1:$2\pi_g$, c_2:$2\pi_g$, c_3:14a, c_4:13b]; (d): C_{11} [d_1:$3\pi_u$, d_2:$3\pi_u$, d_3:$3b_1$, d_4:$13b_2$].

delocalized orbital of π-symmetry (Figures $2a_{1-2}$−d_{1-2}). For the C_5 and C_9 species, the HOMO has *gerade* symmetry under the $D_{\infty h}$ point group (Table 1), which implies that out-of-phase relationships prevail between the extremities of the chains (Figures $1a_{1-2}$, $3a_{1-2}$). Assuming a control of cyclization through the frontier orbitals -a very natural assumption for such nonpolar species-, a torsion should therefore occur to release antibonding overlaps.

The HOMO's of the C_5 and C_9 chains show an *odd*-number (1 or 3, respectively) of nodal planes across the chain (Figures $2a_{1-2}$ and $2c_{1-2}$). Taking account of the out-of-phase relationships that prevail between the extremities of the chains, an *even*-number (2 and 4, respectively) of phase inversions is therefore expected for the two highest occupied molecular orbitals of their cyclic counterparts. The topology of the HOMO in these rings tends to favor significant departures from planarity, since a conjugative pattern of through-space bonding overlaps can develop in the twisted forms, leading to the very peculiar HOMO and HOMO-1 contours of Figures $2a_{3-4}$ and $2c_{3-4}$. At low contour values, these molecular orbitals simply appear in the form of two intertwined tori of opposite sign. These tori are separated by a nodal surface which approximately follows the carbon backbone and shows an *even*-number (2 and 4, respec-

tively) of twists by 180° along the rings. The HOMO's of the cyclic isomers of C_5 and C_9 are therefore fully delocalized and twisted π-orbitals (in short, t-π), which consistently account for both the nonplanar and the cumulenic (i.e., doubly aromatic) nature[24] of these clusters.[19b,c] Notice that the greater part of the electron density contained in these antisymmetric (7b,13b) orbitals lies out of the average molecular plane, which confirms their belonging to the Π-conjugation band system.

The out-of-plane distortions of the ground state molecular structure are noticeably much stronger in the case of C_5 (Figure 1a), which seems to indicate that such distortions are favored by cyclic strains. Looking further in the C_{4n+1} series, one finds indeed that the less strained cyclic isomers of C_{13} and C_{17} are simply planar rings.[19b,c] Nonetheless, and very interestingly, it must be mentioned that the anion form of the C_{13} cyclic cluster is also a twisted torus characterized by *six* phase inversions in its frontier orbitals.[52]

At odds with the C_5 and C_9 species, the *ungerade* symmetry of the HOMO's in the linear forms of C_7 and C_{11} (Table 1) enables a direct in-phase conjugation of the extremities of chains (Figures $2b_{1-2}$, $2d_{1-2}$), which certainly helps in preserving the planarity (Figures 1b, 1d) of their cyclic isomers. The double energy degeneracy of this level is released upon cyclization, yielding one low-lying (HOMO-1) fully delocalized orbital of Π-symmetry (Figures $2b_3$, $2d_3$) and a higher-lying (HOMO) one of Σ symmetry (Figures $2b_4$, $2d_4$). An even-number (2 or 4) of nodal planes is seen across the chain (Figures $2b_{1-2}$, $2d_{1-2}$), which leads correspondingly to an even-number (4 or 6) of phase inversions within the HOMO of the C_7 and C_{11} rings (Figures $2b_4$,$2d_4$), respectively. This orbital shows (Figures $2b_4$,$2d_4$) pronounced localization of the electrons outside the ring, which reflects both the strained and merely polyynic (i.e., doubly antiaromatic) nature of these planar cyclic species.[24]

Upon inspection of the orbital energies reported in Table 1, it appears that the lowest unoccupied molecular orbital (LUMO) of C_5, C_7, C_9, and C_{11} is very substantially destabilized upon ring closure. These cumulenic chains possess as lowest unoccupied level a doubly degenerate and nicely delocalized π-orbital (Figures $3a_{1-2}-d_{1-2}$). Correspondingly, the LUMO of the planar rings (C_7, C_{11}) is also a delocalized orbital of Π-symmetry (Figures $3b_3$, $3d_3$). For the C_7 and C_{11} species, the destabilization of the LUMO which arises upon ring closure can simply be related to the out-of-phase relationships that prevail between the extremities of the chain (Figures $3b_{1-2}$,$3d_{1-2}$). On the other hand, the LUMO's of the cyclic isomers of C_5 and C_9 reflect again very consistently the peculiar topology of these species (Figures $3a_3$, $3c_3$). As for the HOMO, these orbitals consist of two intertwined tori of opposite sign, which display 2 and 4 twists by 180°, respectively. Unlike the HOMO, they are symmetric under the C_2 point group. Compared with the HOMO, a greater part of the electron density associated with the LUMO lies in the average molecular plane. The LUMO of the C_5 and C_9 rings can therefore be regarded as originating from the in-plane ("Σ"-) conjugation band system of these cyclic cumulenic species.

The final outcome of these complex variations in orbital shape and topology upon cyclization is therefore a significant, and at first glance, a rather unexpected increase, by more than 1 eV, of the fundamental (HOMO−LUMO) band gap (Table 1). In comparison with odd-membered linear carbon chains, odd-membered carbon rings are therefore intrinsically characterized by a lower propensity to electronic excitations.

B. Overview of the Ionization Spectra of C_{2n+1} Rings. Results obtained at the HF/cc-pVDZ and 1p-GF/ADC(3)/cc-pVDZ levels for the ionization energies of the C_5, C_7, C_9, C_{11} rings and the related spectroscopic strengths are displayed as spike spectra and in convoluted forms in Figures 4−7a and Figures 4−7b, respectively. The corresponding data are also presented in Tables 2−5.

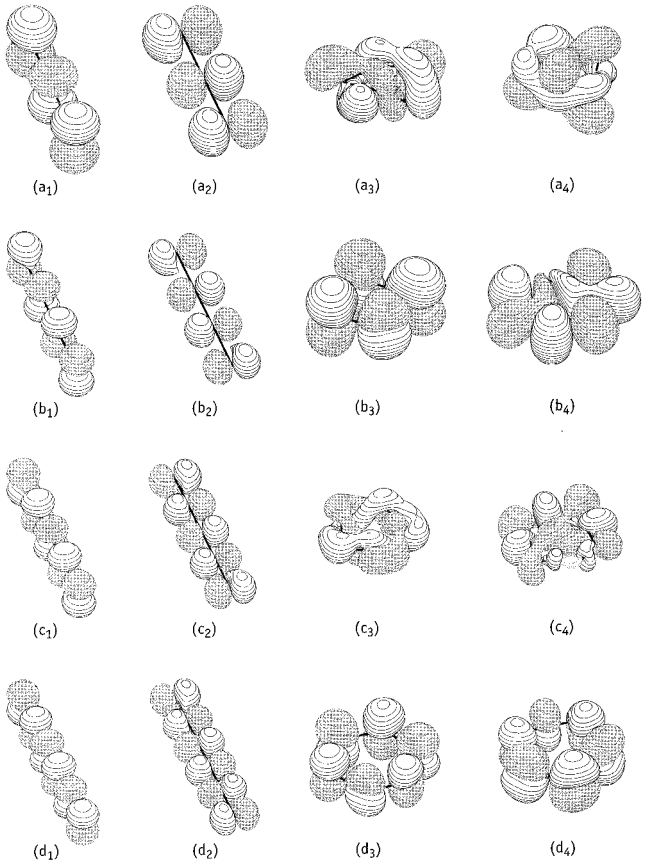

Figure 3. (a_1-d_1, a_2-d_2) Lowest Unoccupied Molecular Orbitals (LUMO) of C_{2n+1} carbon chains versus the (a_3-d_3) LUMO and (a_4-d_4) LUMO+1 orbitals of the C_{2n+1} rings. (a): C_5 [a_1:$2\pi_u$, a_2:$2\pi_u$, a_3:9a, a_4:10a]; (b): C_7 [b_1:$2\pi_g$, b_2:$2\pi_g$, b_3:$3b_1$, b_4:$8b_2$]; (c): C_9 [c_1:$3\pi_u$, c_2:$3\pi_u$, c_3:15a, c_4:16a]; (d): C_{11} [d_1:$3\pi_g$, d_2:$3\pi_g$, d_3:$3a_2$, d_4:$4b_1$].

The HF spectra of C_9 or C_{11} very clearly reflect the partition of the $4n+2$ valence (nondegenerate) orbitals of a large odd-membered C_{2n+1} (n = 4,5) carbon ring into $2n+1$ inner-valence (i.e., C_{2s}) levels at HF binding energies above ∼20 eV, and $2n+1$ levels of dominantly C_{2p} character in the outer-valence region (i.e., at binding energies markedly below 20 eV). This partition can also be inferred from a LCAO analysis or verified through a graphical display of all molecular orbitals. It markedly differs from that unambiguously inferred[22] for the electronic structure of odd-membered C_{2n+1} (n = 2−5) carbon chains, which exhibits $2n$ "C_{2s}" levels and $2n+2$ "C_{2p}" levels at HF electron binding energies above 20 and below 16 eV, respectively. This important difference is consistent with the transformation upon ring closure of the two terminal, highly reactive, and strongly localized lone-pairs of a large cumulenic carbon chain (|C═C·····C═C|) with binding energies of about 13.3 eV[22] into two more stable chemical σ-bonds.

Even at the HF level, the analysis of the electronic structure of the C_{2n+1} rings complicates slightly for the smallest members of the series (C_5, C_7), because of a much stronger energy spreading and partial overlap of the C_{2s} and C_{2p} band systems. This spreading very transparently reflects the enhancement of electron interactions and orbital mixing in highly strained cyclic structures. Therefore, in straightforward analogy with the partition reported previously[23] for the even-membered C_4, C_6

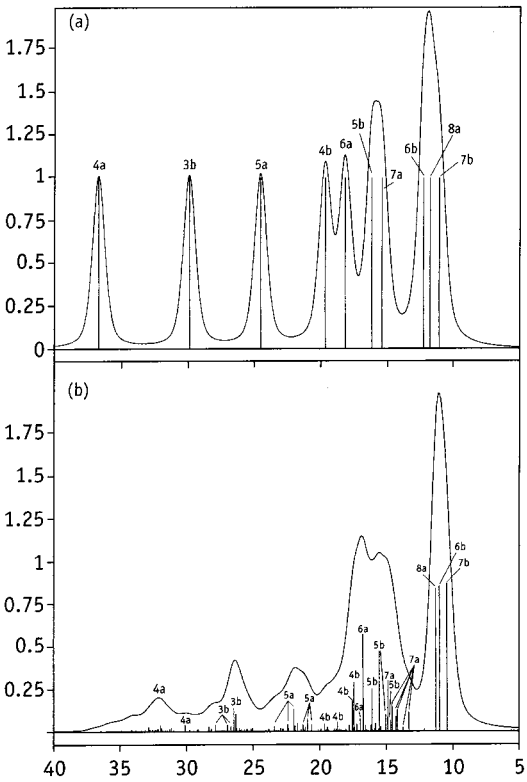

Figure 4. Calculated ionization spectra for the C_5 ring. (a) HF results and (b) ADC(3) results (cc-pVDZ basis set). Pole strengths and convoluted densities of states versus binding energies in eV.

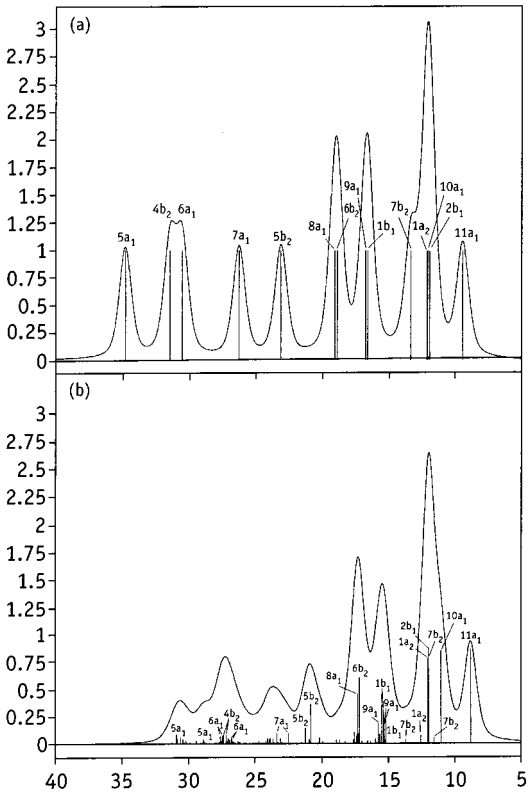

Figure 5. Calculated ionization spectra for the C_7 ring. (a) HF results and (b) ADC(3) results (cc-pVDZ basis set). Pole strengths and convoluted densities of states versus binding energies in eV.

and C_8 rings, and in line with the results of a LCAO analysis, it is more convenient to regard the smallest odd-membered C_{2n+1} rings ($n = 2,3$) as having $2n - 1$ inner-(C_{2s}) and $2n + 3$ outer-

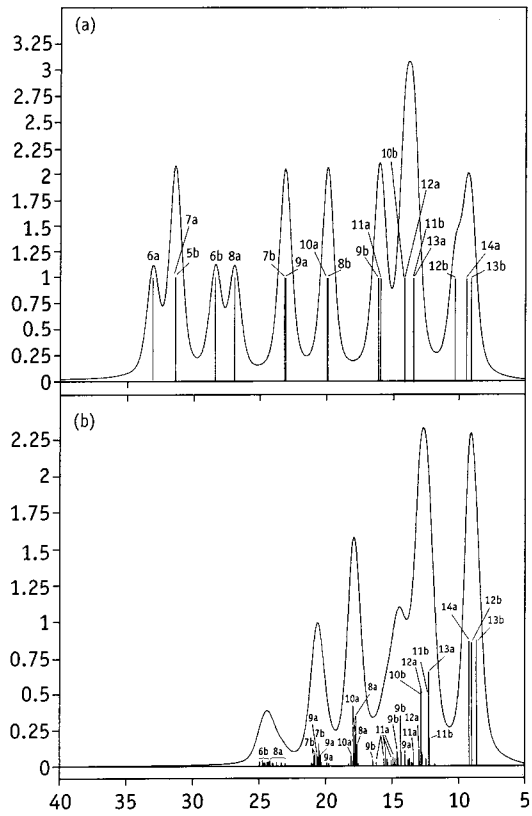

Figure 6. Calculated ionization spectra for the C_9 ring. (a) HF results and (b) ADC(3) results (cc-pVDZ basis set). Pole strengths and convoluted densities of states versus binding energies in eV.

(C_{2p}) valence levels, at binding energies above and below 20 eV, respectively.

As for the carbon chains[22] and rings[23] already studied, inclusion of electronic relaxation, dynamical and static (i.e., nondynamical) correlation and multistate interactions via the 1p-GF/ADC(3) approach results (Figures 1b−4b) in shifts by ∼2 to ∼6 eV of ionization bands toward lower binding energies, together with a very pronounced fragmentation of one-electron ionization lines into complex and very dense sets of low-intensity satellites. The breakdown of the orbital picture of ionization is complete in the inner valence region. It extends down to ionization energies of 10 eV (see further for details), and, quite naturally therefore, leads to substantial band broadening throughout nearly the whole valence region.

Furthermore, electronic relaxation is also occasionally found to yield substantial energy reorderings among the very few one-electron lines that survive the breakdown of the orbital picture. In the planar carbon rings (C_7, C_{11}), many-body effects, electronic relaxation in particular, are found to have a much stronger influence on the one-hole binding energies of the outermost orbitals of σ-symmetry [e.g., $\Delta IP(11a_1/C_7) = -0.717$ eV; $\Delta IP(13b_2/C_{11}) = -1.373$ eV] than on those that exhibit π-symmetry [$\Delta IP(2b_1/C_7) = -0.033$ eV; $\Delta IP(3b_1/C_{11}) = +0.001$ eV]. Such a straightforward discrimination between the outermost levels of the nearly planar C_9 ring can still be made, to some extent (see section III.E) On the other hand, because of the stronger mixing of states due to the symmetry lowering and significant departure from planarity, it does no longer hold for the C_5 ring. In this case, electronic correlation and relaxation are found to result in more homogeneous shifts of the outermost ionization lines [e.g., $\Delta IP(7b/C_5) = -0.627$ eV; $\Delta IP(8a/C_5) = -0.472$ eV].

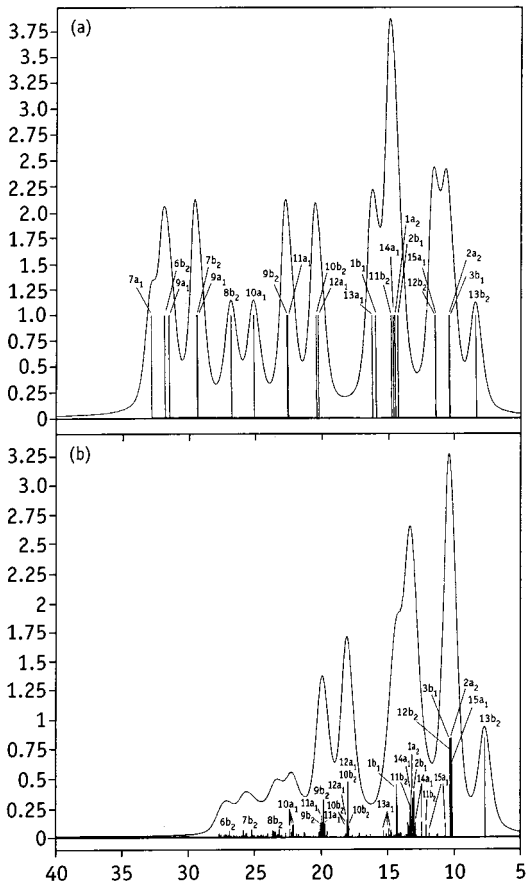

Figure 7. Calculated ionization spectra for the C_{11} ring. (a) HF results and (b) ADC(3) results (cc-pVDZ basis set). Pole strengths and convoluted densities of states versus binding energies in eV.

As is usually the case with low-band gap and rather strongly correlated systems,[22,23,36,38] one can observe overall a rather regular drift of the onset of the satellite bands toward lower binding energies, with increasing system size (C_5: 13.28 eV; C_7: 11.60 eV; C_9: 11.76 eV; C_{11}: 10.62 eV). As usual[22,23,37−43] the breakdown of the orbital picture of ionization dramatically intensifies with system size. In comparison with the odd-membered C_{2n+1} chains,[22] the shake-up fragmentation seen in the computed ionization spectra of the odd-membered C_{2n+1} rings is overall much stronger, despite the increase of the HOMO−LUMO band gap upon ring closure. This is due to the lower symmetry of the rings, which permits many more configuration interactions in the final ionized states. The effect of symmetry lowering can also be assessed from a comparison of the 1p-GF/ADC(3) spectra reported in this work with those obtained previously for the even-membered C_{2n} rings.[23] In any case, the shake-up fragmentation becomes so strong for the C_9 and C_{11} rings that a complete description of the inner-valence region of these species exceeds the current possibilities. For the latter two clusters, it was necessary to restrict the search to ionization lines with a pole strength larger than 0.02, to ensure the convergence of the block-Davidson iterations. This implies that no ionization intensity at all could be recovered for the three innermost valence orbitals of the C_9 and C_{11} rings (i.e., 5b, 7a, 6a; and $7a_1$, $6b_2$, $8a_1$, respectively). Despite these blanks in the simulations and despite the strength of many-body effects, the gross features of the HF electronic structure of the odd-membered carbon rings versus their linear counterparts[22] can still be traced (Figures 4−7) in the energy distribution and shape of the convoluted ADC(3) ionization bands, which justifies the present study and a more detailed analysis of the computed spectra.

C. One-Hole and Shake-Up Ionization Energies of the C_5 Ring. Several trends emerge from the OVGF and ADC(3) results reported for the cyclic isomer of C_5 [Table 2]. Among the 10 valence molecular orbitals of this cluster, only the three outermost ones (7b, 6b, 8a) give rise to ionization lines which can be satisfactorily described on the grounds of a one-electron picture. According to a spreading fwhm parameter of 1.1 eV, these lines cannot be resolved and should result in a rather sharp and intense peak around 10.8 eV (Figure 4b). All Green's Function data undoubtedly confirm Koopmans' assignment of the lowest cation state of the C_5 ring as a ^2B state (IP = ∼10.4 eV). Reordering is observed for the next two levels, 8a and 6b. The latter level relates to an orbital showing significant localization on two nonadjacent carbons, and is thus subject to intense relaxation effects. A comparison of the OVGF values obtained for the $7b^{-1}$, $8a^{-1}$ and $6b^{-1}$ lines also confirms the relatively limited impact on one-electron binding energies of the incompleteness of the cc-pVDZ basis set. Upon consideration of the results displayed in Table 2 and the reasonable assumption of the additivity of the effects of extra split-valence, polarization and diffuse functions, it can be safely stated that the OVGF/cc-pVDZ one-electron binding energies systematically underestimate the OVGF/aug-cc-pVTZ values by ∼0.3 eV, which in turn should be very close to their full basis set limit.

From the 7a orbital and onward, the OVGF and ADC(3) data provide (Table 2) a very different description of ionization bands, due to the rather poor performance of the OVGF method when entering energy regions where shake-up lines normally prevail. According to the ADC(3) results, all one-electron HF energy levels above 15 eV undergo a very strong breakdown of the orbital picture of ionization, whereas the OVGF results provide one-electron ionization lines with a large pole strength ($\Gamma > 0.75$) up to one-electron binding energies of 19.6 eV. However, it should be noticed that the shake-up fragmentation, which is consistently described at the ADC(3) level, can most often be guessed at the OVGF level when the obtained spectroscopic (or pole) strengths (Γ) approach or drop below a value of ∼0.85 (see Table 2). In other words, OVGF pole strengths smaller than ∼0.85 very certainly foretell a significant dispersion of the ionization intensity into secondary two-electron processes. This empirical relationship is verified throughout this work, and can also be very consistently inferred from ample applications of both methods on series of conjugated systems, in particular on polycyclic aromatic hydrocarbons (see the results reported in refs 43 and 53).

Thus, except for the first three outermost valence states, 7b, 8a, and 6b, all ionization lines clearly undergo substantial losses of intensity into shake-up processes. The idea of a one-particle process can be partially retained for ionization of an electron from the 6a level (IP= 16.75 eV), which in the ADC(3) spectrum (Figure 4b) emerges from the shake-up background as an ionization line with dominant one-electron character and appreciable pole strength ($\Gamma = 0.57$), at an ionization energy of 16.7 eV. The onset of the shake-up bands is located at 13.73 eV. Compared with an ADC(3)/cc-pVDZ shake-up ionization threshold of 12.86 eV for the linear isomer,[22] it marks a rather significant withdrawal of shake-up bands in the spectrum, which consistently reflects the larger band gap of the C_5 ring. The shake-up bands extend to the inner-valence region where

TABLE 2: Ionization Potentials (in eV) and Pole Strengths (in parentheses) Obtained for the Cyclic Isomer of C_5 (C_2 Point Group)[a]

level	HF/ cc-pVDZ	ADC(3)/ cc-pVDZ	OVGF/ cc-pVDZ	OVGF/ aug-cc-pVDZ	OVGF/ cc-pVTZ
7b	11.006	10.379 (0.870)	10.233 (0.894)	10.371 (0.888)	10.396 (0.889)
8a	11.703	11.231 (0.842)	10.921 (0.895)	11.057 (0.889)	11.075 (0.890)
6b	12.193	10.945 (0.857)	10.880 (0.888)	11.041 (0.882)	11.073 (0.883)
7a	15.336	13.284 (0.117)	13.984 (0.865)	14.122 (0.859)	14.105 (0.860)
		13.728 (0.025)			
		14.145 (0.134)			
		14.257 (0.094)			
		14.560 (0.174)			
		14.870 (0.301)			
		15.410 (0.032)			
		15.821 (0.052)			
5b	16.110	14.685 (0.066)	15.135 (0.881)	15.265 (0.874)	15.212 (0.875)
		15.044 (0.104)			
		15.517 (0.427)			
		16.080 (0.259)			
6a	18.092	16.148 (0.042)	16.245 (0.824)	16.349 (0.818)	16.352 (0.819)
		16.577 (0.040)			
		16.745 (0.573)			
		16.968 (0.078)			
		17.245 (0.022)			
4b	19.602	17.240 (0.045)	17.269 (0.782)	17.365 (0.775)	17.362 (0.776)
		17.437 (0.294)			
		17.556 (0.192)			
		17.792 (0.040)			
		18.697 (0.058)			
		19.443 (0.030)			
		19.672 (0.046)			
5a	24.489	20.655 (0.044)			
		20.981 (0.079)			
		21.148 (0.029)			
		21.300 (0.043)			
		21.709 (0.050)			
		21.909 (0.036)			
		22.003 (0.138)			
		22.398 (0.020)			
		22.470 (0.046)			
		23.015 (0.021)			
		23.479 (0.033)			
3b	29.853	25.124 (0.022)			
		25.244 (0.020)			
		26.111 (0.021)			
		26.317 (0.022)			
		26.382 (0.108)			
		26.517 (0.143)			
		26.747 (0.033)			
		27.020 (0.041)			
		27.901 (0.043)			
		28.407 (0.031)			
4a	36.640	30.201 (0.044)			
		31.214 (0.024)			
		31.939 (0.022)			
		32.027 (0.038)			
		32.926 (0.030)			

[a] Only the lines with $\Gamma > 0.02$ are listed.

ionization lines are smashed into an extremely large number of lines with very small intensity.

Despite the importance of the shake-up fragmentation, the gross features of the one-electron HF band structure (Figure 4a) are still clearly apparent in the convoluted ADC(3) ionization spectrum of the cyclic isomer of C_5. This spectrum strongly differs from that previously calculated for its linear counterpart (see Figure 2c of ref 22). Despite the increase of the band gap, the shake-up fragmentation is by far stronger for the cyclic isomer of C_5 than for the linear one, because of the much lower symmetry (C_2) of the former species. The obtained ADC(3) results indicate that more than 40% of the inner-valence ionization intensity of the C_5 ring is lost into satellites with a pole strength less than 0.005, whereas these lines "only" amount to 29% of the C_{2s} ionization intensity of the five-membered carbon chain. For the latter species, the idea of a one-particle ionization process could actually be partially retained[22] for two of the four inner-valence levels.

D. One-Hole and Shake-Up Ionization Energies of the C_7 Ring. By far and large, many conclusions drawn for the ADC-(3) and OVGF ionization spectra of the C_5 ring straightforwardly apply to the C_7 one. Here also, a comparison of the ADC(3) and OVGF results (Table 3) confirm the rule that OVGF pole strengths less than ~0.85 are indicative of a breakdown of the orbital picture of ionization. In this case, only the three outermost ionization lines can be safely described as one-electron lines. The obtained OVGF results also confirm the adequacy of the cc-pVDZ basis set.

TABLE 3: Ionization Potentials (in eV) and Pole Strengths (in parentheses) for the Cyclic Isomer of C_7 (C_{2v} Point Group)[a]

level	HF/ cc-pVDZ	ADC(3)/ cc-pVDZ	OVGF/ cc-pVDZ	OVGF/ aug-cc-pVDZ	OVGF/ cc-pVTZ	level	HF/ cc-pVDZ	ADC(3)/ cc-pVDZ
$11a_1$ (Σ)	9.521	8.804 (0.872)	8.703 (0.895)	8.868 (0.890)	8.862 (0.891)	$7a_1$ (Σ)	26.376	22.570 (0.103)
$2b_1$ (Π)	12.027	11.994 (0.874)	11.903 (0.894)	12.010 (0.887)	12.043 (0.887)			23.078 (0.024)
$10a_1$ (Σ)	12.171	11.060 (0.861)	10.831 (0.883)	10.986 (0.878)	10.954 (0.879)			23.166 (0.057)
$1a_2$ (Π)	12.219	12.049 (0.787)	12.022 (0.896)	12.128 (0.888)	12.168 (0.889)			23.330 (0.024)
		12.597 (0.083)						23.436 (0.104)
$7b_2$ (Σ)	13.441	11.604 (0.062)	11.781 (0.856)	11.928 (0.851)	11.924 (0.851)			23.704 (0.020)
		11.989 (0.698)						23.743 (0.049)
		13.704 (0.048)						23.936 (0.056)
		14.123 (0.020)						24.000 (0.056)
$1b_1$ (Π)	16.674	14.810 (0.043)	15.054 (0.818)	15.185 (0.811)	15.113 (0.812)			24.034 (0.042)
		15.271 (0.039)						24.152 (0.057)
		15.369 (0.316)						24.262 (0.034)
		15.497 (0.361)						24.807 (0.033)
		18.955 (0.044)						26.299 (0.021)
$9a_1$ (Σ)	16.831	15.210 (0.230)	15.155 (0.823)	15.307 (0.817)	15.237 (0.817)	$6a_1$ (Σ)	30.636	26.230 (0.026)
		15.321 (0.138)						26.352 (0.024)
		15.665 (0.094)						26.398 (0.030)
		15.792 (0.198)						26.691 (0.024)
		15.985 (0.054)						26.808 (0.047)
		16.630 (0.020)						26.856 (0.058)
		18.714 (0.042)						27.267 (0.049)
		19.993 (0.024)						27.517 (0.020)
$6b_2$ (Σ)	18.970	16.363 (0.031)	16.874 (0.823)	17.024 (0.804)	16.934 (0.804)			27.551 (0.075)
		17.040 (0.032)						27.706 (0.076)
		17.213 (0.612)						27.811 (0.021)
		17.326 (0.028)				$4b_2$(Σ)	31.548	26.809 (0.026)
		17.416 (0.031)						27.007 (0.039)
		17.457 (0.077)						27.113 (0.056)
$8a_1$ (Σ)	19.157	16.593 (0.039)	16.935 (0.832)	17.082 (0.822)	17.038 (0.835)			27.172 (0.030)
		17.276 (0.101)						27.272 (0.086)
		17.345 (0.463)						27.474 (0.089)
		17.407 (0.097)						27.623 (0.033)
		17.599 (0.113)						28.896 (0.028)
		17.679 (0.046)						29.491 (0.032)
		18.302 (0.025)				$5a_1$ (Σ)	34.886	28.950 (0.047)
$5b_2$ (Σ)	23.217	20.211 (0.063)						30.265 (0.035)
		20.244 (0.048)						30.497 (0.049)
		20.875 (0.370)						30.664 (0.070)
		20.948 (0.026)						30.898 (0.053)
		20.990 (0.048)						30.979 (0.095)
		21.287 (0.152)						31.299 (0.020)
		21.489 (0.020)						
		21.581 (0.021)						

[a] Only the lines with $\Gamma > 0.02$ are listed.

Examination of the ADC(3) and OVGF ionization energies of the C_7 cyclic species demonstrate that the Koopmans' assignment of the lowest cation state to a $^2A_1$ state is correct. According to all results obtained, this state should appear in the ionization spectrum (Figure 5) as a nicely isolated one-electron line, at a strikingly low binding energy (IP = 8.80 eV, at the ADC(3) level), reflecting both the importance of cyclic strains and the strong impact of electronic relaxation on states derived from ionization of a σ-orbital in a planar structure. Here also, ADC(3) indicates permutations among the next four levels ($10a_1$, $7b_2$, $2b_1$, and $1a_2$) with respect to the Hartree−Fock energy order. Beyond these levels, all orbitals undergo a significant breakdown of the orbital picture of ionization. In this case, the onset of the shake-up bands lies at an electron binding energy near 11.6 eV. The orbital picture of ionization is partially restored at the bottom of the outer-valence region, in the form of two lines at 17.2 and 17.3 eV with appreciable one-electron character ($\Gamma = 0.61$, $\Gamma = 0.46$), which relate to the $6b_2$ and $8a_1$ orbitals, respectively. As for the C_5 ring, the fragmentation into satellites intensifies with increasing ionization energies, in particular in the inner-valence region, where the orbital picture of ionization fully breaks down. However, despite the larger size of the cyclic C_7 species, the shake-up fragmentation appears to be significantly less acute than the one which occurs in the case of C_5. This observation relates to the larger symmetry (C_{2v}) of the C_7 ring, which helps to limit the number of permitted initial- and final-state configuration interactions. Compared with C_5 (Figure 4b), sharper and better resolved peaks therefore quite naturally emerge in the convoluted ADC(3) ionization spectrum of the cyclic isomer of C_7 (Figure 5b). In this case, the (unrecovered) part of the inner-valence intensity relating to satellites with a pole strength less than 0.005 is around 34%. This can be compared with a dispersion into such satellites of 29% of the C_{2s} ionization intensity of the linear form of C_7. For the latter species, despite a lower band gap, the higher symmetry ($D_{\infty h}$) indeed permits a partial preservation of the one-electron picture of ionization[22] in the inner-valence region, in the form of four lines with a pole strength larger than 0.40.

E. One-Hole and Shake-Up Ionization Energies of the C_9 Ring. Compared with the first term of the C_{4n+1} series, C_5, the onset of the shake-up band of the C_9 ring has been reduced by nearly 2 eV to a value of 11.76 eV (Table 4), which is qualitatively in line with the changes observed in the band gap from one species to the other (Table 1). Due to its more pronounced planarity, one can in this case rather easily assess the belonging of the nine outermost C_{2p} orbitals of this

TABLE 4: Ionization Potentials (in eV) and Pole Strengths (in parentheses) for the Cyclic Isomer of C_9 (C_2 Point Group)[a]

level	HF/ cc-pVDZ	ADC(3)/ cc-pVDZ	OVGF/ cc-pVDZ	OVGF/ aug-cc-pVDZ	level	HF/ cc-pVDZ	ADC(3)/ cc-pVDZ
13b (t−π)	9.066	8.605 (0.868)	8.331 (0.888)	8.455 (0.882)	10a	19.961	17.778 (0.220)
14a (t−π)	9.437	9.170 (0.864)	8.660 (0.884)	8.794 (0.879)			17.873 (0.091)
12b (t−σ)	10.300	8.965 (0.854)	9.023 (0.877)	9.169 (0.872)			17.904 (0.275)
13a (t−σ)	13.439	11.759 (0.020)	12.043 (0.836)	12.175 (0.831)			17.932 (0.035)
		12.206 (0.655)					18.044 (0.073)
11b (t−σ)	13.457	12.135 (0.199)	12.051 (0.838)	12.182 (0.833)			18.071 (0.074)
		12.223 (0.503)					18.263 (0.022)
		13.473 (0.025)			9a	23.119	19.760 (0.024)
		14.016 (0.025)					19.900 (0.027)
12a (t−π)	14.115	12.428 (0.055)	12.483 (0.814)	12.600 (0.807)			20.336 (0.030)
		12.777 (0.507)					20.366 (0.083)
		12.903 (0.040)					20.414 (0.058)
		12.951 (0.122)					20.483 (0.062)
		13.549 (0.030)					20.595 (0.069)
10b (t−π)	14.132	12.740 (0.101)	12.490 (0.814)	12.604 (0.807)			20.648 (0.068)
		12.799 (0.544)					20.666 (0.088)
		12.967 (0.040)			7b	23.214	20.378 (0.033)
		13.545 (0.025)					20.503 (0.161)
		15.294 (0.031)					20.529 (0.065)
11a ($\sim\sigma$)	15.946	13.378 (0.103)	14.150 (0.795)	14.284 (0.789)			20.557 (0.023)
		13.685 (0.058)					20.789 (0.094)
		13.787 (0.049)					20.846 (0.040)
		13.992 (0.028)					20.887 (0.078)
		14.528 (0.063)					20.962 (0.021)
		14.640 (0.071)					21.061 (0.024)
		14.754 (0.042)			8a	26.968	23.068 (0.024)
		14.926 (0.066)					23.328 (0.024)
		15.059 (0.043)					23.377 (0.024)
		15.377 (0.051)					23.724 (0.034)
		15.507 (0.132)					23.971 (0.021)
		15.616 (0.059)					24.025 (0.026)
		16.182 (0.031)					24.212 (0.041)
9b ($\sim\pi$)	16.118	14.045 (0.087)	14.156 (0.806)	14.272 (0.799)			24.280 (0.031)
		14.329 (0.357)			6b	28.426	24.275 (0.024)
		14.618 (0.106)					24.344 (0.037)
		14.782 (0.057)					24.401 (0.025)
		14.799 (0.028)					24.436 (0.031)
		14.836 (0.026)					24.567 (0.026)
		16.455 (0.046)					24.618 (0.026)
		17.520 (0.042)					24.680 (0.027)
8b	19.907	17.610 (0.042)		17.548 (0.812)			24.779 (0.042)
		17.624 (0.155)					25.001 (0.033)
		17.696 (0.352)					25.019 (0.036)
		17.738 (0.049)			5b	31.418	
		17.871 (0.080)			7a	31.442	
		17.889 (0.062)			6a	33.114	
		17.930 (0.036)					

[a] Only the lines with $\Gamma > 0.02$ are listed.

cumulenic ring (Figure 2c_{3-4}; Figures 8a−g) to the Π- and Σ-conjugation band systems. With regard to their dominant out-of-plane orientation, the 13b (HOMO), 14a (HOMO-1), 12a, 10b orbitals displayed in Figures 2c_4, 2c_3, 8d, and 8e should rather be related to twisted (t-) π levels, whereas the 12b, 13a, 11b orbitals (Figures 8a−c) more markedly belong to the "Σ-" (in-plane) band system. By extension, they will therefore be described as twisted (t-) σ levels (Table 4). The two remaining C_{2p} levels, 11a and 9b, clearly relate (Figure 8f,g) to the Σ- and Π- band systems, respectively.

All theoretical data provide the ^{2}B state as lowest cation state, at a binding energy of 8.61 eV. Notice that this ionization threshold is practically the same as that found for the standard C_7 ring, an observation which nicely reflects the attenuation of electronic relaxation and the lower impact of cyclic strains on t-π orbitals. Here also, a reordering of the ionization energies is seen for the next two orbitals, 14a and 12b, due to the stronger impact of electronic relaxation on the latter t-σ level. However, as for the C_5 cumulenic ring (and unlike the C_7 polyynic cyclic species), the three outermost lines cannot be resolved according to our convolution (fwhm = 1.1 eV), and result therefore into a sharp and intense peak at ∼9.0 eV (Figure 6b).

Except for the three outermost ionization lines at ionization energies below 9 eV, with a pole strength larger than 0.8, all ionization lines have a pronounced shake-up character. The orbital picture of ionization can nonetheless be partially retained at higher binding energies, in the form of four ionization lines emerging clearly from the shake-up background at 12.21 eV ($\Gamma = 0.66$), 12.22 eV ($\Gamma = 0.50$), 12.78 eV ($\Gamma = 0.51$) and 12.80 eV ($\Gamma = 0.54$), and relating to the 13a, 11b, 12a, and 10b orbitals, respectively. Beyond these lines, the breakdown of the orbital picture of ionization can be regarded as complete because the obtained pole strengths do not exceed 0.36. The shake-up fragmentation very quickly intensifies with increasing ionization energies, due to the lower symmetry (C_2) of the C_9 ring.

Despite the intensification of the shake-up fragmentation and the missing contributions of the three innermost orbitals (5b, 7a and 6a), the identified ADC(3) ionization lines fall in very well-resolved sets (Figure 6b), which by their total intensity

TABLE 5: Ionization Potentials (in eV) and Pole Strengths (in parentheses) for the Cyclic Isomer of C_{11} (C_{2v} Point Group, cc-pVDZ Basis Set)[a]

level	HF	ADC(3)	OVGF	level	HF	ADC(3)
$13b_2$ (Σ)	8.963	7.590 (0.858)	7.489 (0.886)	$12a_1$ (Σ)	20.181	17.943 (0.061)
$3b_1$ (Π)	10.271	10.272 (0.852)	10.053 (0.880)			17.969 (0.049)
$2a_2$ (Π)	10.320	10.156 (0.860)	10.144 (0.880)			18.014 (0.478)
$15a_1$ (Σ)	11.333	10.096 (0.632)	9.971 (0.852)			18.073 (0.151)
		10.619 (0.125)				18.110 (0.039)
		11.243 (0.029)		$10b_2$ (Σ)	20.343	17.917 (0.101)
		11.861 (0.037)				18.011 (0.421)
$12b_2$ (Σ)	11.363	10.240 (0.777)	9.941 (0.857)			18.051 (0.125)
		11.196 (0.030)				18.090 (0.093)
		11.288 (0.020)				18.204 (0.036)
$2b_1$ (Π)	14.182	12.986 (0.399)	12.821 (0.815)	$11a_1$ (Σ)	22.484	19.593 (0.053)
		13.101 (0.027)				19.769 (0.118)
		13.255 (0.108)				19.787 (0.027)
		13.356 (0.070)				19.876 (0.069)
		13.434 (0.078)				19.891 (0.107)
		14.245 (0.051)				19.953 (0.035)
		14.846 (0.023)				19.981 (0.188)
		18.101 (0.026)				20.192 (0.047)
$1a_2$ (Π)	14.399	12.825 (0.022)	12.842 (0.811)	$9b_2$ (Σ)	22.554	19.577 (0.029)
		13.047 (0.035)				19.859 (0.330)
		13.083 (0.343)				19.875 (0.141)
		13.141 (0.032)				20.091 (0.123)
		13.205 (0.111)		$10a_1$ (Σ)	25.059	21.262 (0.036)
		13.312 (0.129)				21.316 (0.044)
		14.033 (0.043)				21.740 (0.027)
		14.232 (0.031)				21.896 (0.033)
$14a_1$ (Σ)	14.538	12.423 (0.134)	12.797 (0.824)			22.127 (0.112)
		12.880 (0.127)				22.217 (0.103)
		13.191 (0.411)				22.291 (0.045)
		13.599 (0.028)				22.390 (0.073)
		14.136 (0.034)		$8b_2$ (Σ)	26.770	22.415 (0.038)
$11b_2$ (Σ)	14.686	12.072 (0.109)	12.800 (0.808)			22.750 (0.038)
		12.942 (0.060)				23.007 (0.020)
		13.270 (0.278)				23.213 (0.070)
		13.411 (0.105)				23.316 (0.027)
		13.479 (0.129)				23.366 (0.020)
		14.363 (0.024)				23.493 (0.046)
		14.682 (0.044)				23.516 (0.039)
		16.611 (0.021)				23.601 (0.053)
$1b_1$ (Π)	15.854	13.957 (0.036)	13.928 (0.805)			23.737 (0.058)
		14.228 (0.085)				24.090 (0.032)
		14.272 (0.105)				24.393 (0.020)
		14.317 (0.455)		$9a_1$ (Σ)	29.306	
		14.699 (0.026)		$7b_2$ (Σ)	29.364	24.579 (0.020)
		14.732 (0.034)				25.245 (0.021)
$13a_1$ (Σ)	16.136	14.174 (0.027)	14.056 (0.793)			25.324 (0.069)
		14.254 (0.278)				25.664 (0.036)
		14.310 (0.083)				25.736 (0.021)
		14.749 (0.066)				25.759 (0.030)
		14.908 (0.077)				25.912 (0.023)
		15.075 (0.031)				25.939 (0.061)
		15.126 (0.031)		$8a_1$ (Σ)	31.443	
		15.312 (0.056)		$6b_2$ (Σ)	31.776	26.991 (0.055)
		16.292 (0.029)				27.188 (0.021)
		17.130 (0.037)				27.929 (0.027)
						27.598 (0.024)
						27.739 (0.033)
				$7a_1$ (Σ)	32.779	

[a] Only the lines with $\Gamma > 0.02$ are listed.

and energy distribution rather clearly recall the outermost part of the HF spectrum (Figure 6a). As a matter of fact, compared with the C_5 cyclic species, the convoluted shake-up bands remain much sharper, reflecting an overall weaker energy dispersion of the computed 2h-1p ionized states. The same observation was made previously[38] when comparing the ADC(3) spectra of cyclohexane and cyclopentane with that of cyclobutane,[38] and seems therefore to indicate a release of cyclic strains in larger carbon rings.

F. One-Hole and Shake-Up Ionization Energies of the C_{11} Ring. Except for the contribution of the two innermost orbitals of a_1 symmetry, the ADC(3) ionization spectrum of the cyclic isomer of C_{11} has been nearly entirely recovered. Like with the C_7 polyynic ring (and at odds with the ADC(3) ionization spectra of the cumulenic C_5 and C_9 rings), the outermost ionization line ($13b_2^{-1}$) is very well separated from the rest of the spectrum (Figure 7b), and falls at a strikingly low binding energy (7.6 eV), owing again to the impact of cyclic strains and of electronic relaxation on levels of Σ symmetry in planar species. Here also, only three ionization lines with binding energies larger than 10 eV can be safely assigned to one-hole ionized states ($13b_2^{-1}$, $3b_1^{-1}$, $2a_2^{-1}$). A partial preservation of the orbital picture of ionization can also be considered for the next two levels, $15a_1$ and $12b_2$. These relate to orbitals of Σ symmetry, and as such

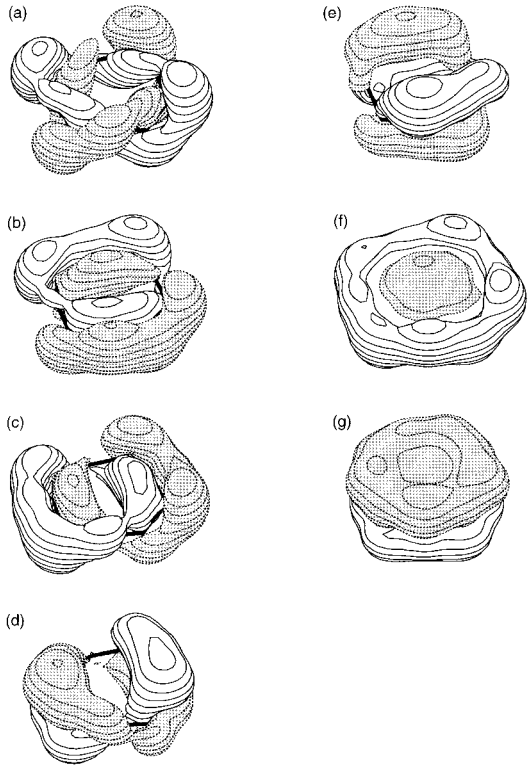

Figure 8. Outer-valence (C_{2p}) orbitals of the C_9 ring. By order of increasing energy: (a) 12b (HOMO-2), (b) 13a, (c) 11b, (d) 12a (e), 10b, (f) 11a and (g) $5a_g$. The HOMO-1 (14a) and HOMO (13b) levels are displayed in Figures $2c_3$ and $2c_4$, respectively.

undergo much stronger relaxation effects upon ionization than the two above lying Π-levels, $3b_1$ and $2a_2$. As a result, at odds with the HF eigenspectrum (Figure 7a), the $3b_1$, $2a_2$, $15a_1$, and $12b_2$ levels are nearly accidentally degenerate in the ADC(3) ionization spectrum, and lead therefore to a strikingly sharp and intense peak near ~10.1 eV.

Except from this difference, and despite the severity of the shake-up fragmentation of bands beyond this point, the basic features of the HF electronic structure (Figure 7a) are easily recognizable in the ADC(3) ionization spectrum (Figure 7b), in the investigated range of electron binding energies. Here also, upon a comparison with the results obtained for the smallest odd-membered polyynic carbon cluster, C_7, the band broadening due to the splitting of lines into shake-up sets appears to be more limited, in line with the idea[38] that this splitting provides an indirect measure of structural strains in cyclic compounds.

IV. Conclusions and Outlook for the Future

The present investigation of the electronic structure and ionization properties of odd-membered carbon rings shows that "magic rules" can still be found in theoretical studies of so highly versatile and challenging species. Both structurally and electronically, the cyclic C_5 and C_9 clusters have to be described as *even-twisted cumulenic tori*. These species are nonplanar structures characterized by an even-number of phase inversions in their frontier orbitals. On the contrary, the cyclic isomers of the C_7 and C_{11} species are simply *planar polyynic rings*. This topological distinction between cyclic members of the C_{4n+1} or C_{4n+3} series ($n = 1,2$) is consistent with the *gerade* or *ungerade* character of the HOMO in their linear counterparts, respectively. It leads to highly significant fingerprints in the ionization spectra of these odd-membered carbon rings.

As for the linear C_{2n+1} and cyclic C_{2n+2} clusters ($n = 1-4$) investigated previously,[22,23] many body effects (correlation, relaxation, multi-configurational mixing) have a considerable influence on the vertical ionization spectra of odd-membered carbon rings. Compared with the linear species, these display an intrinsically lower propensity to electronic excitations, in the form of a significantly larger HOMO−LUMO band gap. On the other hand, the lower symmetry of the C_{2n+1} rings ($n = 1-4$), C_5 and C_9 in particular, results into many more configuration interactions in the cation. The ultimate outcome of these two opposite factors is overall a severe enhancement of the shake-up fragmentation of ionization bands, compared with the odd-membered chains.

Despite the extent of the shake-up contamination, the present study undoubtedly confirms that structural fingerprints in ionization spectra could be usefully exploited to discriminate the cyclic and linear isomers of odd-membered C_{2n+1} clusters in plasma conditions. Such spectra could even be used to indirectly trace very fine details of the molecular structure, such as the alternation of bond lengths. For instance, the highest occupied level of the C_5 and C_9 rings relates to a twisted and nicely delocalized π-orbital, which is in line with their relatively high ionization potential. On the other hand, the vertical ionization threshold of the polyynic and planar carbon rings C_7 and C_{11} corresponds to a rather strongly localized orbital of σ-symmetry, appearing thereby at strikingly low binding energies in the ionization spectrum. At last, the extent of cyclic strains can also be indirectly evaluated through the energy dispersion of shake-up lines, which directly influences the apparent broadening of bands.

With regard to the extent of the structural information borne in these spectra, it would certainly be worth refining the ADC-(3) treatment of vertical ionization processes, which relies on a single-reference ground state wave function. Besides coping with multireference effects, one should also put in perspective the role played by the higher-order shake-up (3h-2p, 4h-3p,...) transitions, which are neglected at this level of theory. Inclusion of diffuse and continuum functions in the basis sets should also be considered to account more consistently for shake-up transitions toward Rydberg states, as well as their shake-off limit. At last, it would also be worth assessing at reliable theoretical levels the impact of the twists of π-chemical bonds on electron affinities.[52]

Acknowledgment. The authors acknowledge financial support from the "Bijzonder Onderzoeksfonds" (BOF) of the Limburgs Universitair Centrum. M.S.D is also grateful to the "Fonds voor Wetenshappelijk Onderzoek − Vlaanderen", the Flemish Science Foundation, for additional funding. He is indepted to Prof. L. S. Cederbaum (Heidelberg University, Germany) for continuous support and training in Green's Function theory (1995-2001). The authors would like to thank Dr. A. B. Trofimov (Irkutsk University, Russian federation) for his kind help.

References and Notes

(1) (a) Weltner, W., Jr.; Van Zee, R. J. *Chem. Rev.* **1989**, *89*, 1713. (b) Weltner, W., Jr.; Van Zee, R. J. *J. Mol. Structure (THEOCHEM)* **1990**, *222*, 201.

(2) Van Orden, A.; Saykally, R. J. *Chem. Rev.* **1998**, *98*, 2313.

(3) (a) Bollick, E. A.; Ramsey, D. A. *Astrophys. J.* **1963**, *137*, 84. (b) Kroto, H. W. *Int. Rev. Phys. Chem.* **1981**, *1*, 309. (c) Bell, M. B.; Feldman, P. A.; Kwok, S.; Matthews, H. E. *Nature (London)* **1982**, *389*, 295. (e) Krätschmer, W.; Nachtigall, K. in *Polycyclic Aromatic Hydrocarbons and Astrophysics*; edited by A. Lèger et al.; Reidel: Dordrecht, 1987. (d) Hinkle, K. H.; Keady, J. J.; Bernath, P. F. *Science* **1988**, *241*, 1319. (e) Bernath, P.

F.; Hinkle, K. H.; Keady, J. J. *Science* **1989**, *244*, 562. (f) Cermak, I.; Monninger, G.; Krätschmer, W. *Advances in Molecular Structure Research*; JAI Press: 1997; Vol. 3, pp 117−146.

(4) (a) Edwards, J. B. *Combustion: Formation and Emission of Trace Species*; Ann. Arbor Science: Ann. Arbor, MI, 1974. (b) Zhang, Q. L.; O'Brien, S. C.; Heath, J. R.; Liu, Y.; Curl, R. F.; Kroto, H. W.; Smalley, R. E. *J. Phys. Chem.* **1986**, *90*, 525. (c) Kroto, H. W.; McKay, K. *Nature* **1988**, *331*, 328.

(5) (a) *ZFI Mitteilungen*, nr. *134*: *Beiträge zur Clusterforschung*, Academie der Wissenschaften der DDR, September 1987. (b) Celii, F. G.; Butler, J. E. *Annu. Rev. Phys. Chem.* **1991**, *42*, 643. (d) Curl, R. F. *Rev. Mod. Phys.* **1997**, *69*, 691.

(6) Levy Guyer, R.; Koshland, D. E., Jr. *Science* **1990**, *250*, 1640.

(7) (a) Kroto, H. W.; Walton, D. R. M. *The Fullerenes. New Horizons for the Chemistry, Physics and Astrophysics of Carbon*; Cambridge University Press: New York, 1993. (b) Dresselhaus, M. S.; Dresselhaus, G.; Eklund, P. C. *Science of Fullerenes and Carbon Nanotubes*; Academic Press: New York, 1996. (c) Kroto, H. *Rev. Mod. Phys.* **1997**, *69*, 703. (e) Smalley, R. F. *Rev. Mod. Phys.* **1997**, *69*, 723.

(8) (a) Iijima, S. *Nature* **1991**, *354*, 56. (b) Iijima, S.; Achihashi, T.; Ando, Y.; *Nature* **1992**, *356*, 776. (c) Ajayan, P. M.; Iijima, S. *Nature* **1992**, *358*, 23. (d) Ebbesen, T. W.; Ajayan, P. M. *Nature* **1992**, *358*, 220. (e) Amelincks, S.; Zhang, X. B.; Bernaerts, D.; Zhang, X. F.; Ivanov, V.; Nagy, J. B.; Lucas, A. A.; Lambin, Ph. *Science* **1994**, *265*, 635.

(9) Hare, J. P.; Hsu, W. K.; Kroto, H. W.; Lappas, A.; Prassides, K.; Terrones, M.; Walton, D. R. M. *Chem. Mater.* **1996**, *8*, 6.

(10) Tast, F.; Malinowski, N.; Billas, I. M. L.; Heinebrodt, M.; Branz, W.; Martin, T. P. *J. Chem. Phys.* **1997**, *17*, 6980.

(11) (a) Raghavachari, K.; Binkley, J. S. *J. Chem. Phys.* **1987**, *98*, 2191. (b) Raghavachari, K.; Curtiss, L. A. "Accurate Theoretical Studies of Small Elemental Clusters". In *Quantum Mechanical Electronic Structure Calculations with Chemical Accuracy*; Langhoff, S. R., Ed.; Kluwer: Dordrecht, 1995. (c) Shlyakhter, Y.; Sokolova, S.; Lüchow, A.; Anderson, J. B. *J. Chem. Phys.* **1999**, *110*, 17 025.

(12) Bernholdt, D. E.; Magers, D. H.; Bartlett, R. J. *J. Chem. Phys.* **1988**, *89*, 3612.

(13) Watts, J. D.; Gauss, J.; Stanton, J. F.; Bartlett, R. J. *J. Chem. Phys.* **1992**, *97*, 8372.

(14) Martin, J. M. L.; François, J. P.; Gijbels, R.; Almlöf, J. *Chem. Phys. Lett.* **1991**, *187*, 367.

(15) Hutter, J.; Lüthi, H. P.; Diederich, F. *J. Am. Chem. Soc.* **1994**, *116*, 750.

(16) Hutter, J.; Lüthi, H. P. *J. Chem. Phys.* **1994**, *101*, 2213.

(17) Pless, V.; Suter, H. U.; Engels, B. *J. Chem. Phys.* **1994**, *101*, 4042.

(18) Martin, J. M. L.; Taylor, P. R. *J. Phys. Chem.* **1996**, *100*, 6047.

(19) (a) Martin, J. M. L.; François, J.-P.; Gijbels, R. *J. Chem. Phys.* **1990**, *93*, 8850. (b) Martin, J. M. L.; El-Yazal, J.; François, J. P. *Chem. Phys. Lett.* **1995**, *242*, 570. (c) Martin, J. M. L.; El-Yazal, J.; François, J. P. *Chem. Phys. Lett.* **1996**, *252*, 9.

(20) Gotts, N. G.; von Helden, G.; Bowers, M. T. *Int. J. Mass. Spectrom. Ion Processes* **1995**, *149/150*, 217, and references therein.

(21) Vager, Z.; Feldman, H.; Kella, E.; Malkin, E.; Miklazky, E.; Zajfman, J.; Naaman, R. *Z. Phys. D − Atoms, Molecules and Clusters* **1991**, *19*, 413.

(22) Deleuze, M. S.; Giuffreda, M. G.; François, J.-P.; Cederbaum, L. S. *J. Chem. Phys.* **1999**, *111*, 5851.

(23) Deleuze, M. S.; Giuffreda, M. G.; François, J.-P.; Cederbaum, L. S. *J. Chem. Phys.* **2000**, *112*, 5325.

(24) Giuffreda, M. G.; Deleuze, M. S.; François, J.-P. *J. Phys. Chem. A* **1999**, *103*, 5137.

(25) Trinajstic, N. *Chemical Graph Theory*; CRC Press: Boca Raton, Florida, 1983; Vol. I, chapter VI.

(26) Cederbaum, L. S.; Schirmer, J.; Domcke, W.; von Niessen, W. *Adv. Chem. Phys.* **1986**, *65*, 115.

(27) Cederbaum, L. S. *J. Phys. B: Atom. Mol. Phys.* **1975**, *8*, 290.

(28) von Niessen, W.; Schirmer, J.; Cederbaum, L. S. *Comput. Phys. Rep.* **1984**, *1*, 57.

(29) Ortiz, J. V. *J. Chem. Phys.* **1988**, *89*, 6348.

(30) Schirmer, J.; Cederbaum, L. S.; Walter, O. *Phys. Rev. A* **1983**, *28*, 1237.

(31) Schirmer, J.; Angonoa, G. *J. Chem. Phys.* **1989**, *91*, 1754.

(32) Weikert, H.-G.; Meyer, H.-D.; Cederbaum, L. S.; Tarantelli, F. *J. Chem. Phys.* **1996**, *104*, 7122.

(33) Cederbaum, L. S.; Domcke, W. *Adv. Chem. Phys.* **1977**, *36*, 205 and references therein.

(34) Szabo, A.; Ostlund, N. S. *Modern Quantum Chemistry*; Macmillan: New York, 1982.

(35) (a) Linderberg, J.; Öhrn, Y. *Propagators in Quantum Chemistry*; Academic Press: London, 1973. (b) Öhrn, Y.; Born, G. *Adv. Quantum Chem.* **1981**, *13*, 1. (c) Öhrn, Y. in *Lecture Notes in Chemistry*; Mukherjee, D., Ed.; 1988; Vol 50, 185−206.

(36) Pickup, B. T.; Goscinski, O. *Mol. Phys.* **1973**, *26*, 1013. Ortiz, J. V. in *Computational Chemistry: Reviews of Current Trends*; Leszczyinski, J., Ed.; World Scientific: Singapore, 1997; Vol. 2, p 1.

(37) Deleuze, M. S.; Cederbaum, L. S. *Phys. Rev. B* **1996**, *53*, 13326.

(38) Deleuze, M. S.; Cederbaum, L. S. *J. Chem. Phys.* **1996**, *105*, 7583.

(39) Deleuze, M. S.; Cederbaum, L. S. *Int. J. Quantum Chemistry* **1997**, *63*, 465.

(40) Deleuze, M. S.; Cederbaum, L. S. *Adv. Quantum. Chem.* **1999**, *35*, 77.

(41) Golod, A.; Deleuze, M. S.; Cederbaum, L. S. *J. Chem. Phys.* **1999**, *110*, 6014.

(42) Deleuze, M. S.; Giuffreda, M. G.; François, J.-P.; Cederbaum, L. S. *J. Phys. Chem. A* **2000**, *104*, 1588.

(43) Deleuze, M. S.; Trofimov, A. B.; Cederbaum, L. S. *J. Chem. Phys.* **2001**, *115*, 5859.

(44) (a) Parr, R. G.; Wang, W. *Density-Functional Theory of Atoms and Molecules*; Oxford University Press: New York, 1989. (b) Koch, W.; Holthausen, M. C. *A Chemist's Guide to Density Functional Theory*, Second Edition; Wiley-VCH: Weinheim, 2001.

(45) (a) Becke, A. D. *J. Chem. Phys.* **1993**, *98*, 5648. (b) Lee, C.; Yang, W.; Parr, R. G. *Phys. Rev. B* **1988**, *37*, 785.

(46) Dunning, T. H., Jr. *J. Chem. Phys.* **1989**, *90*, 1007.

(47) Martin, J. M. L.; El-Yazal, J.; François, J.-P. *Mol. Phys.* **1995**, *86*, 1437.

(48) Frisch, M. J.; Trucks, G. W.; Schlegel, H. B.; Scuseria, G. E.; Robb, M. A.; Cheeseman, J. R.; Zakrzewski, V. G.; Montgomery, J. A.; Stratmann, R. E.; Burant, J. C.; Dapprich, S.; Millam, J. M.; Daniels, A. D.; Kudin, K. N.; Strain, M. C.; Farkas, O.; Tomasi, V.; Barone, V.; Cossi, M.; Cammi, R.; Mennucci, B.; Pomelli, C.; Adamo, C.; Clifford, S.; Ochterski, J.; Petersson, G. A.; Ayala, P. Y.; Cui, Q.; Morokuma, K.; Malick, D. K.; Rabuck, A. D.; Raghavachari, K.; Foresman, J. B.; Cioslowski, J.; Ortiz, J. V.; Stefanov, B. B.; Liu, G.; Liashenko, A.; Piskorz, P.; Komaromi, I.; Gomberts, R.; Martin, R. L.; Fox, D. J.; Keith, T.; Al-Laham, M. A.; Peng, C. Y.; Nanayakkara, A.; Gonsalez, C.; Challacombe, M.; Gill, P. M. W.; Johnson, B. G.; Chen, W.; Wong, M. W.; Andres, J. L.; Head-Gordon, M.; Replogle, E. S.; Pople, J. A. *Gaussian 98*, revision A.7; Gaussian Inc.: Pittsburgh, PA, 1998.

(49) (a) Kendall, R. A.; Dunning, T. H., Jr.; Harrison, R. J. *J. Chem. Phys.* **1992**, *96*, 6796. (b) Woon, D. E.; Dunning, T. H., Jr. *J. Chem. Phys.* **1993**, *98*, 1358.

(50) Using the original ADC(3) code developed in Heidelberg by Walter, O.; Schirmer, J.; Cederbaum, L. S.; Angonoa, G.; Weikert, H.-G.; Scheller, M. K.; ...; improved by Trofimov, A. B.

(51) Schmidt, M. W.; Baldridge, K. K.; Boatz, J. A.; Jensen, J. H.; Koseki, S.; Gordon, M. S.; Nguyen, K. A.; Windus, T. L.; Elbert, S. T. *QCPE Bull.* **1990**, *10*, 52.

(52) Giuffreda, M. G.; Deleuze, M. S.; François, J. P. "*Structural, Rotational, Vibrational and Electronic Properties of Carbon Cluster Anions C_n^- (n = 3−13)*", submitted for publication in *J. Phys. Chem. A.*

(53) Deleuze, M. S. *J. Chem. Phys.* **2002**, *116*, 7012.